Dynamics of Proteins in Different Solvent Systems: Analysis of Essential Motion in Lipases

G. H. Peters,*# D. M. F. van Aalten,§ O. Edholm,¶ S. Toxvaerd,* and R. Bywater#
*Chemistry Department III, H. C. Ørsted Institutet, University of Copenhagen, DK-2100 Copenhagen Ø, Denmark; #Novo-Nordisk A/S, DK-2880 Bagsvaerd, Denmark; §Department of Biochemistry and Molecular Biology, University of Leeds, Leeds LS2 9JT, UK; and ¶Theoretical Physics, Royal Institute of Technology, S-10044 Stockholm, Sweden

ABSTRACT We have investigated the effect of different solvents on the dynamics of *Rhizomucor miehei* lipase. Molecular dynamics simulations were performed in water, methyl hexanoate, and cyclohexane. Analysis of the 400-ps trajectories showed that the solvent has a pronounced effect on the geometrical properties of the protein. The radius of gyration and total accessibility surface decrease in organic solvents, whereas the number of hydrogen bonds increases. The essential motions of the protein in different solvents can be described in a low-dimensional "essential subspace," and the dynamic behavior in this subspace correlates with the polarity of the solvent. Methyl hexanoate, which is a substrate for *R. miehei* lipase, significantly increases the fluctuations in the active-site loop. During the simulation, a methyl hexanoate entered the active-site groove. This observation provides insight into the possible docking mechanism of the substrate.

INTRODUCTION

Lipases (acylglycerol acylhydrolase, EC 3.1.1.3) are very diverse in their enzymatic properties and substrate specificities, which make possible a wide range of industrial applications. A large number of lipases have been screened for application as industrial reagents (stereospecific synthesis of compounds, transesterification), food additives (flavor modifying enzymes), stain removers (detergent additives), and medical compounds (digestive drugs) (Vulfson, 1994).

The overall catalytic process involves adsorption of the enzyme from the bulk aqueous phase to the surface of and catalysis in the water-lipid interface (Brockman, 1984). The proposed reaction scheme is based on a surface-mediated mechanism (Muderhwa and Brockman, 1992), because a dramatic rise in lipolytic activity is observed when the level of water-insoluble substrates exceeds the critical micelle concentration (Verger et al., 1984; Piéroni et al., 1990). Understanding of the action of lipases has made much progress as a result of the determination of the three-dimensional crystal structures of several lipases (Derewenda et al., 1994; Brzozowski et al., 1991), including the inactive and active forms of the lipase-inhibitor complexes. The three-dimensional structure of *Rhizomucor miehei* lipase-inhibitor complex (Brzozowski et al., 1991; Derewenda et al., 1992a) has been used as a model for the interfacial activation of lipases. The crystal structures revealed that the lipases contain a catalytic center with a trypsin-like triad [Ser-. . .His. . .Asp], which is shielded from the solvent by an α-helical loop ("the lid"). Conformational changes observed during the activation of lipases range from a relatively simple, rigid-body, hinge-type motion of a single helix to much more complex reorganization of multiple lids (Derewenda et al., 1994), as it is seen in human pancreatic (Lawson et al., 1994), *Geotrichum candidum* (Schrag et al., 1993), and *Candida rugosa* (Grochulski et al., 1993) lipases. During activation, the lid is displaced to allow access of the substrate to the active site. From the crystal structures it is evident that not only does the backbone of the central part of the lid move by more than 7 Å, but the accessible hydrophobic surface also increases by approximately 750 Å^2 (Derewenda et al., 1992a). This agrees well with the general observation that, in an aqueous solution, the lipase activity is increased in the presence of a lipid interface (Verger et al., 1984; Piéroni et al., 1990). In an aqueous solution, the opening of the lid is presumably thermodynamically unfavorable, because of a large hydrophobic patch that would necessarily be exposed as a result. Conversely, in the presence of hydrophobic interfaces, such as substrate lipid micelles, this nonpolar surface would be favored, and hence the open conformation of the lid would be stabilized.

Theoretical descriptions of the catalytic process are based either on a surface-mediated mechanism ("substrate theory"), which suggests that the preexisting surface structure of the lipid substrate may have considerable influence on the behavior of lipolytic enzymes, or on the conformational changes in the enzyme upon adsorption to the interface ("enzyme theory") (Peters et al., 1995b; Derewenda et al., 1994; Thuren, 1988). As shown by earlier studies (Muderhwa and Brockman, 1992; Peters et al., manuscript submitted for publication), these models are merely conceptual extremes and are not mutually exclusive. The interfacial character of the lipid/water phase as well as the distribution of charged residues on the enzyme surface, influences the lipase action. Lipase activation is enhanced by the formation of salt links between charged residues in the lid and protein (Peters et al., 1996). Lateral lipid distribution may increase

Received for publication 26 March 1996 and in final form 5 August 1996.
Address reprint requests to Dr. G. H. Peters, H. C. Oersted Institute, Chemistry Department 3, University of Copenhagen, Universitets parken 5, DK-2100 Copenhagen Oe, Denmark. Tel.: 45-35-320236; Fax: 45-35-320259; E-mail: ghp@st.ki.ku.dk.

0006-3495/96/11/2245/11 $2.00

or inhibit lipolytic hydrolysis (Jain and Berg, 1989; Ransac et al., 1990). For instance, inhibition of lipases due to the presence of fatty acid may be explained by repulsive charge-charge interactions between fatty acid moieties in the lipid layer, and charged residues at the enzyme surface essentially prevent the adsorption of the enzyme (Peters et al., manuscript submitted for publication).

Enzymatic reactions occur in aqueous media because life evolved with water as the primary solvent, and an aqueous environment is optimal for maintaining the catalytically active conformations of the enzyme for binding and catalysis. However, in recent years, it has become apparent that a variety of enzymes, including lipases, are catalytically active in apolar solvents (Gupta, 1992). An important prerequisite for this application was the recognition that lipases work in organic solvents with low water content. Under given experimental conditions, the amount of water in the reaction mixture will determine the direction of the lipase-catalyzed reaction. With water absent, or present in trace quantities only, esterification and transesterification are favored, whereas with excess water, hydrolysis occurs. It has been postulated (Zaks and Klibanov, 1988) that the main role of water is to form bonds with functional groups on the protein. In the absence of water, or in mixtures with limited amounts of water, the properties of lipases depend strongly on solvents and incubation conditions (Goldberg et al., 1990; Gupta, 1991; Aldercreutz and Mattiasson, 1987; Khmelnitsky et al., 1988), and catalytic rate, thermostability, selectivity, and "molecular memory" can markedly change in different solvents. Biochemical activities are probably controlled by structural changes and/or by changes in the motion of flexible loops (Kempner, 1993; Philippopoulos et al., 1995; Falzone et al., 1994; Williams and McDermott, 1995) or, in general, concerted motion (Amadei et al., 1993; van Aalten et al., 1995) in enzymes.

An understanding of the mechanistic basis of these phenomena is important for designing new enzymes by genetic engineering techniques. One approach, which has been described in the literature, is to perform molecular dynamics simulations of proteins in organic solvent and aqueous solution and compare the protein conformations (Norin et al., 1994; Fitzpatrick et al., 1993; De Loof et al., 1992; Lautz et al., 1990; Hartsough and Merz, 1993). Conclusions regarding enzyme properties were based on static quantities such as the number of hydrogen bonds, secondary structure, radius of gyration, etc. In the present study, we have focused on the dynamic aspect and have analyzed the concerted motions in *Rhizomucor miehei* lipase (Rml) when it is simulated in hydrophobic or hydrophilic environments. Simulations were performed in water and the organic solvents methyl hexanoate and cyclohexane. It is well established that the catalytic reaction occurs in the lipid-water interphase. Lipases have very low activity in water, when the substrate concentration is below the critical micelle concentration for the substrate. Upon activation, the lid is displaced by several ångstrøms. It is exactly this motion along the activation pathway which, at the present time, is difficult to probe by experiment, but about which computer simulations might provide essential information. Typical motions of peptide loops occur on time scales of 10^{-9} to 10^{-1} s (Wade et al., 1993; Wade et al., 1994; Kempner, 1993; Philippopoulos et al., 1995; Falzone et al., 1994; Williams and McDermott, 1995), which at the present time are not accessible with standard molecular dynamics (MD), when the protein is modeled in full atomic detail. It is exactly this area in which essential dynamics provide an avenue for studying the motions along the activation pathway, and which may enhance our understanding of the dynamics of the protein as it binds to the lipid interface. The effect of a lipid interface on the activation of Rml might be elucidated by studying the changes in dynamics in different solvents.

MODEL AND SIMULATION DETAILS

Molecular dynamics

The high-resolution crystal structure of the native Rml, solved to 1.9-Å resolution (Derewenda et al., 1992b), was used as the model for the inactive structure. Coordinates were obtained from the Protein Data Bank at Brookhaven (Bernstein et al., 1977) (entry code: 3tgl). The secondary structure of the native Rml shown in Fig. 1 is composed of a central β-sheet system of nine strands. The structure is stabilized by three disulfide bridges.

Simulations were performed under different conditions to investigate the effect of the polarity of the solvent on the dynamics in Rml. Simulations were carried out in water (4438), methyl hexanoate (533), and cyclohexane (1135)

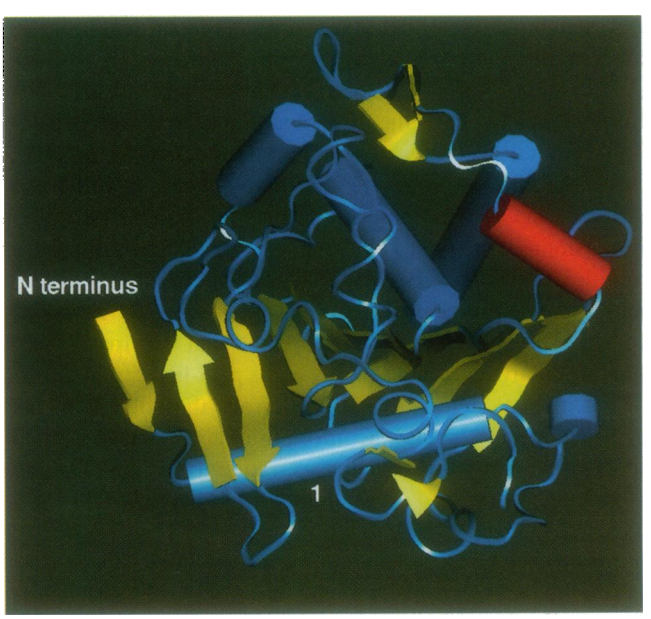

FIGURE 1 Secondary structure of the inactive conformation of the *Rhizomucor miehei* lipase. Sheets and helices are represented by the arrows (*yellow*) and cylinders, respectively. The red cylinder is the helical lid covering the active serine.

(numbers given in parentheses correspond to the number of solvent molecules). Cyclohexane was modeled as a Lennard-Jones fluid. The Lennard-Jones potential parameters are $\sigma = 5.6$ Å and $\epsilon/k_B = 385$ K (Liem, 1992), where k_B is the Boltzmann constant. All simulations were performed using the GROMOS program (van Gunsteren and Berendsen, 1987). The C version (charged) and the D version (uncharged) of the GROMOS force field were used in the simulations with polar and nonpolar solvents, respectively. In addition, the effect of the force field on the results was tested by carrying out simulations with methyl hexanoate using the C version of the GROMOS force field. In this simulation, only internal, buried residues were charged (Arg80, Arg178, Arg196, Asp203, Glu220, and Glu221). Periodic boundary conditions were applied in all simulations. In the simulation of the Rml in aqueous solution, single point charge water taken from a liquid equilibrium configuration (Berendsen et al., 1987) was added to the box, and 11 water molecules at the lowest electrostatic potential were replaced by sodium ions to neutralize the system. The system was equilibrated for 5 ps using a temperature coupling constant of 0.01 ps and a pressure coupling constant of 0.05 ps. The nonbonded pair list was updated every 10 steps, and the nonbonded and long-range electrostatic interactions were truncated at 8 Å and 10 Å, respectively. The SHAKE algorithm (Ryckaert et al., 1977) was applied to constrain the bond lengths to their equilibrium positions, and the equations of motion were solved using the Verlet algorithm (Allen and Tildesley, 1992). Simulations were performed at 300°K with a time step of 2 fs. Examinations of the molecular structures and analyses of the trajectories were carried out using the WHAT IF modeling program (Vriend, 1990).

The simulations of methyl hexanoate were started from a well-equilibrated trajectory (Norin et al., 1994). Methyl- and methylene groups were modeled as united atoms, where the hydrogen atoms are modeled by an increased van der Waals radius of the carbon atoms. In the simulation with organic solvent, all residues carrying net charges were neutral and were treated as dipoles (Norin et al., 1994). Other simulations were started from the crystallographic structure of Rml and subjected to a steepest descents energy minimization until no significant energy change could be detected. This was followed by a 5-ps startup run taking the initial velocities from a Maxwellian distribution at 300°K. Simulations were run for 400 ps, and coordinates were saved every 0.05 ps. The last 300 ps of the trajectory were stable, as estimated by the evaluation of several geometrical properties. These 300-ps trajectories were used for the essential dynamics analysis.

Essential dynamics

The essential dynamics method (Amadei et al., 1993) is based on the diagonalization of the covariance matrix built from atomic fluctuations in a trajectory from which overall translation and rotations have been removed:

$$\mathbf{M} = \langle (X_i - X_{i,0})(X_j - X_{j,0}) \rangle, \quad (1)$$

in which X are the separate x, y, z coordinates of the atoms, fluctuating around their average positions X_0. $\langle \ldots \rangle$ denotes an average over time. The diagonalization of this matrix using the QL algorithm (Press et al., 1987) yields a set of eigenvectors and corresponding eigenvalues. The eigenvectors describe directions in the $3N$ configurational space, representing correlated positional changes of groups of coordinates. The eigenvalues indicate the total mean square fluctuation along these directions. As a matter of convention, the eigenvectors are ordered by the size of their corresponding eigenvalues, i.e., the first eigenvector is the eigenvector with the largest eigenvalue. The central hypothesis of essential dynamics is that only the eigenvectors with large corresponding eigenvalues are important for describing the overall motion of the protein. In general it has been shown for several proteins (Amadei et al., 1993; van Aalten et al., 1996a, b) that taking the first 10 eigenvectors represents about 95% of the total motion of the protein. Projection of the trajectory on a certain eigenvector (by simply calculating the inner product) allows a study of the time dependence of the motion along this eigenvector. In addition, this dot product may be used to generate a structure, by taking the average structure (calculated over the whole trajectory) and then adding to each coordinate the product of the dot product and the corresponding component from the eigenvector. In this way, the average structure is displaced along the direction of that eigenvector, the distance of the displacement being indicated by the size of the dot product.

A useful method for comparing the essential dynamics of two simulations on similar systems is the so-called combined analysis (van Aalten et al., 1995). In this method, two or more trajectories fitted on the same reference structure are concatenated, and a covariance matrix is constructed. The trajectory is then projected onto the resulting eigenvectors, and the properties of these projections are compared for all simulations. There are two main effects to be studied: 1) the differences in average projection, indicating that simulations have different average displacements along eigenvectors, i.e., have a different equilibrium structure in that direction; 2) differences in the mean square fluctuation in the projection, indicating a difference in dynamics along this direction. Here this method is applied to the concatenated trajectories of the water, methyl hexanoate, and cyclohexane simulations.

RESULTS AND DISCUSSION

The stability of the simulations was checked by computing several geometrical quantities, which are displayed in Fig. 2. The changes in the radius of gyration (R_G) and number of hydrogen bonds (N_H) (Fig. 2 *a*) reflect the polarity of the solvents. With decreasing polarity (water → methyl hexanoate → cyclohexane), R_G decreases (≈1.667 → ≈1.635

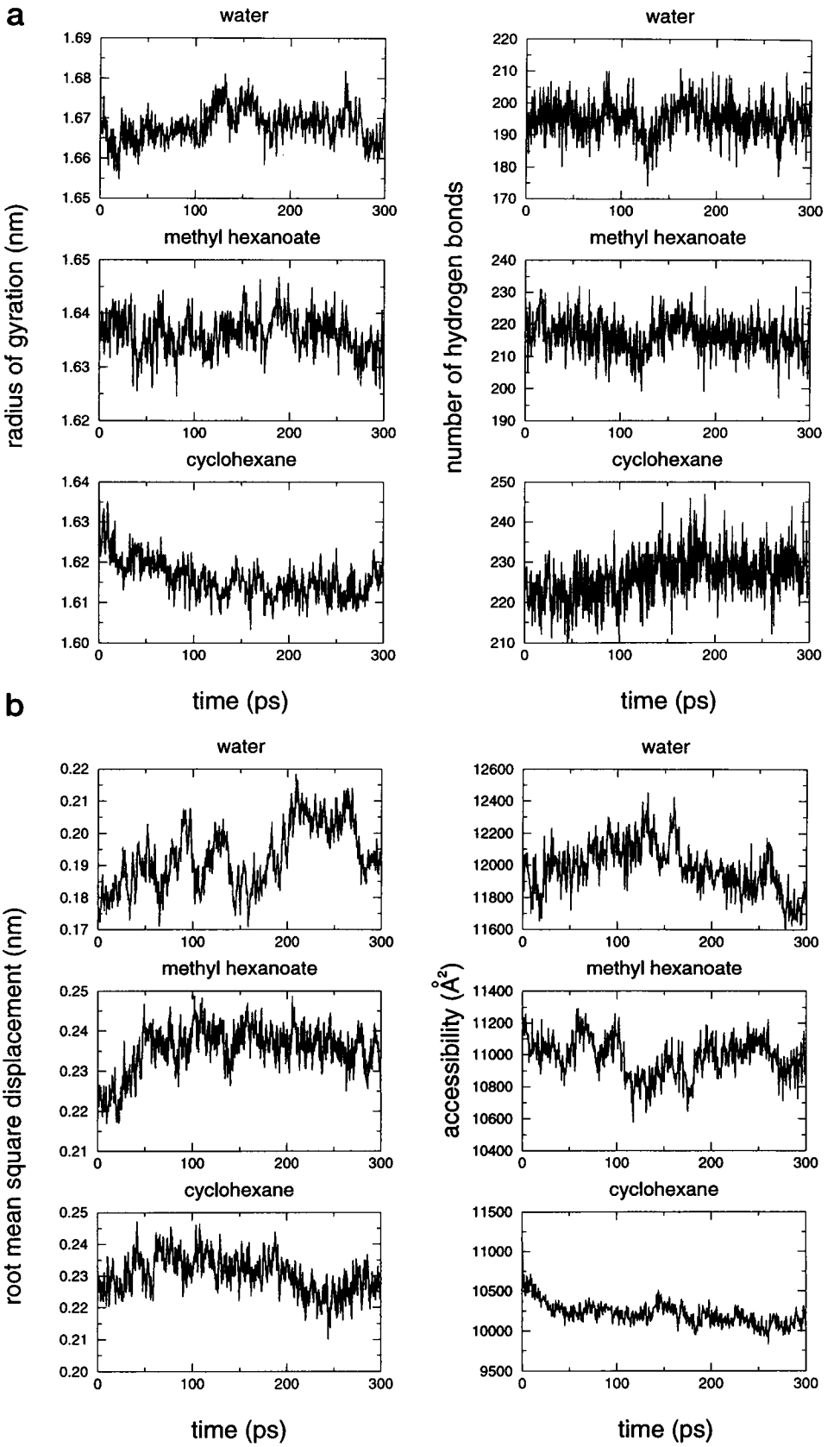

FIGURE 2 Geometrical properties calculate during the simulations with different solvents. (*a*) Radius of gyration and number of hydrogen bonds as a function of time. (*b*) Root mean square displacement (rmsd) and accessibility as a function of time. Rmsd's were calculated between the crystal structure of the inactive form and the structures obtained during the course of the simulations. Surface accessibility was calculated with DSSP (Kabsch and Sander, 1983).

$\rightarrow \approx 1.615$) and N_H increases ($\approx 195 \rightarrow \approx 215 \rightarrow \approx 227$). The observed changes might be caused by the folding back of the charged side chains onto the protein surface in a nonpolar solvent (Norin et al., 1994; Hartsough and Merz, 1993). The structure is stabilized by an increase in the number of hydrogen bonds. This effect also reflects the decrease in the surface accessibility ($\approx 11850 \rightarrow \approx 11000 \rightarrow \approx 10125$), and the larger deviations from the crystal structure for the simulations with organic solvents (see Fig. 2 *b*). In short, the results above indicate that we have obtained stable trajectories that can be used for essential dynamics analyses.

The main analysis performed in this study is the determination of the essential dynamics properties. The trajectories obtained from the simulations were first analyzed independently. The cumulative normalized eigenvalues as a function of eigenvector indices are shown in Fig. 3. The original $3N$-dimensional configurational space formed by the C_α coordinates consists of 795 vectors ($3N$ C_α; N = 265). The eigenvectors obtained from the essential dynamics analysis describe directions in this space, representing a certain motion in the protein. The eigenvalues indicate the contribution of the corresponding eigenvector to the overall motion in the protein. As shown in Fig. 3, only a few eigenvectors are needed to describe the essential motions in the protein; approximately 80% of the total motion is described by the first 40 eigenvectors. This shows that most of the internal motion of the Rml can be represented by a subspace that is much smaller than original $3N$ configurational space. Slight differences are observed for the solvents, and in general, more eigenvectors are needed to describe a certain percentage of the total positional fluctuations in nonpolar solvent than in polar solvent.

The differences in dynamics in the trajectories were studied by performing a combined analysis of the three concatenated trajectories. Differences in the essential subspace can be studied by projecting the separate trajectories onto the "combined" eigenvectors. The average of the projections and the mean square fluctuations in these projections as a function of eigenvector indices are shown in Fig. 4. As explained in the previous section, the average projection shows differences in equilibrium structure, whereas the mean square fluctuation can be used to study differences in dynamics. In addition, eigenvector motions are visualized in Fig. 5, and absolute values of the first four eigenvectors as a function of residue number are shown in Fig. 6. In general, as observed before for other proteins, the protein core (especially the active site) is rather rigid, with flexible loops (including the lid) on the surface. Significant differences are observed at several eigenvectors (see Fig. 4). The large change in structure shown by eigenvector 1 (see Figs. 4 *a*, 5 *a*, and 6 *a*) can be attributed to a "shrinking" of the protein by organic solvents. In nonpolar solvent, the loop Gly35-Ile52, which connects the N-terminus with a β-sheet, folds

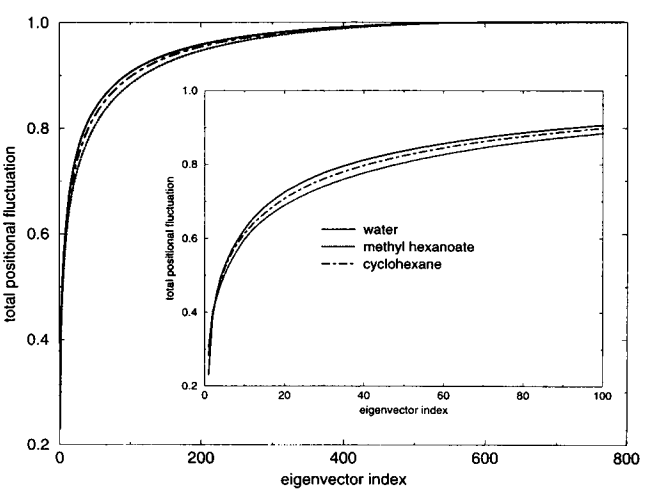

FIGURE 3 Total positional fluctuations as a function of eigenvector indices computed from the C_α covariance matrix for the different solvents.

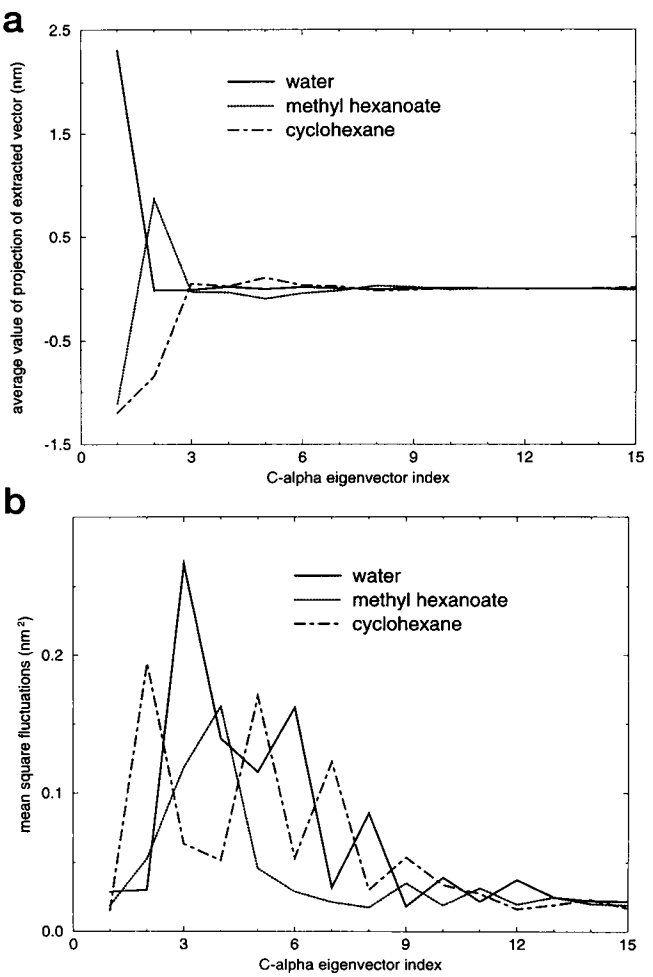

FIGURE 4 (*a*) Average values of the projections of the extracted vectors obtained from the C_α coordinate covariance matrix of the concatenated trajectories of Rml in different solvents as a function of the eigenvector index. (*b*) Mean square fluctuations of the values of the projections of the extracted vectors obtained from the C_α coordinate covariance matrix of the concatenated trajectories of the different solvents as a function of the eigenvector index.

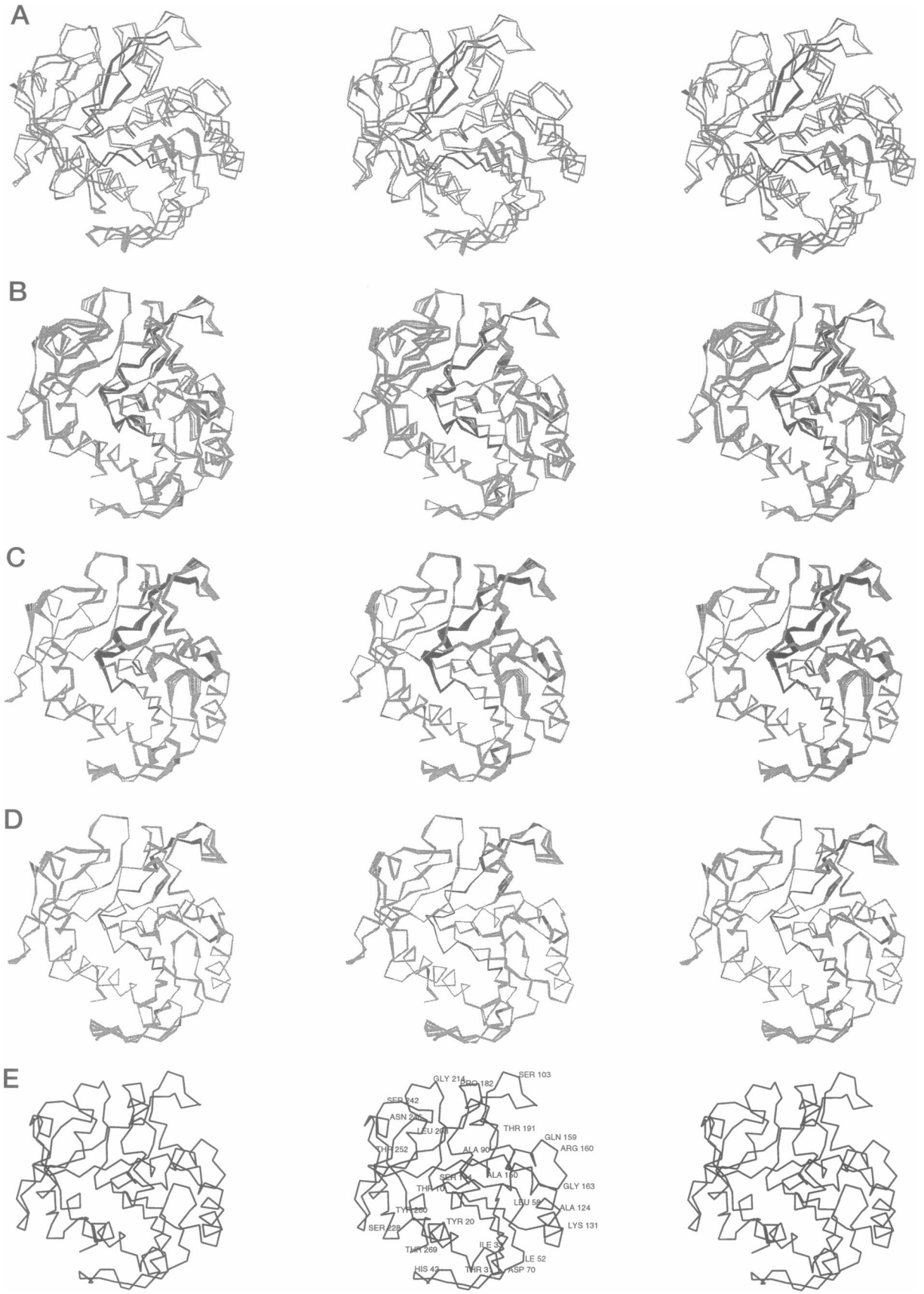

FIGURE 5 Superposition of 10 configurations obtained by projecting the C_α motion onto the first four eigenvectors (*a–d*). (*e*) C_α trace of native Rml displaying selected residues and residue numbers. Configurations are separated by 30 ps.

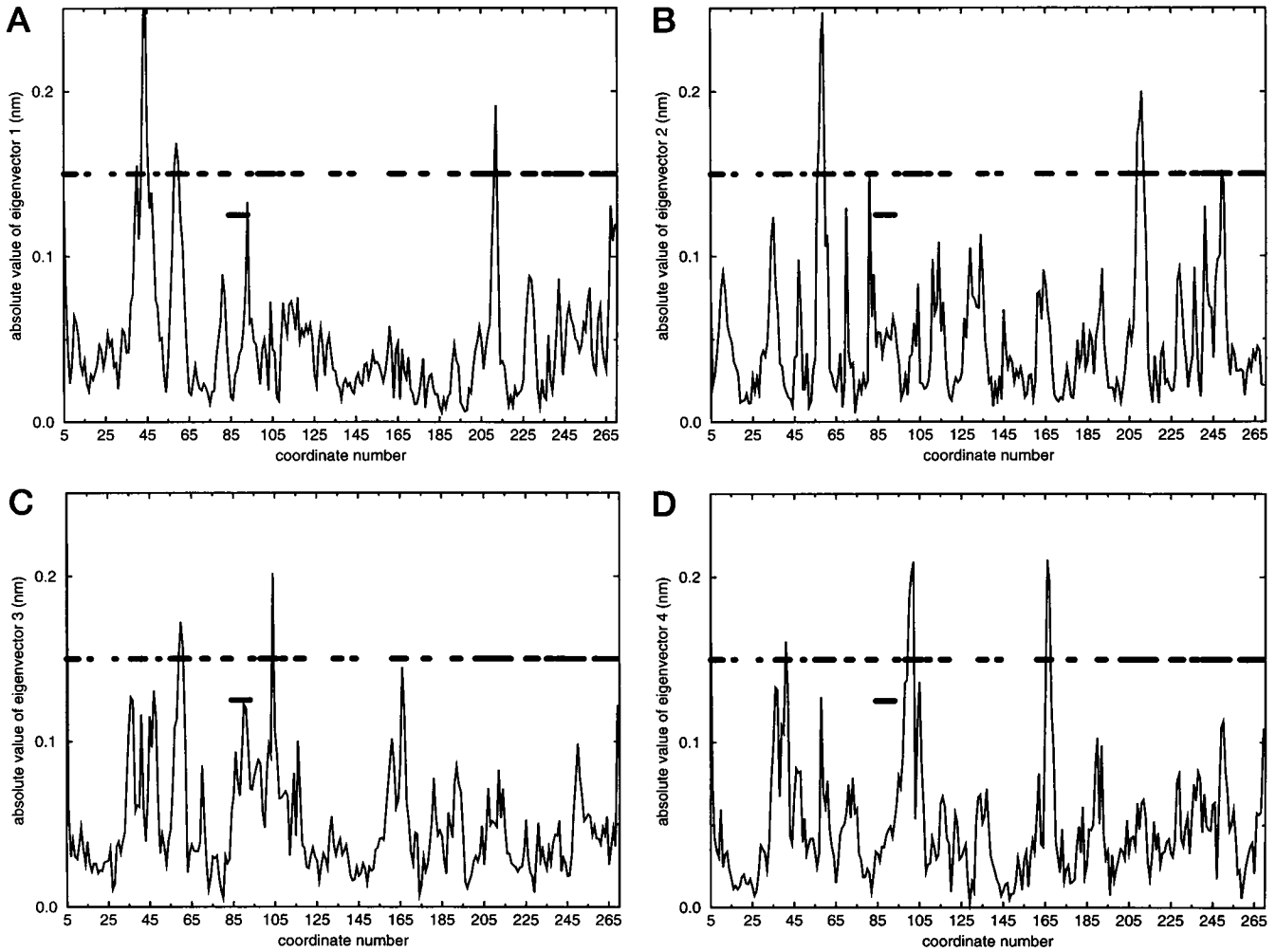

FIGURE 6 Absolute value of the components of the first four eigenvectors (*a–d*) obtained from the C_α coordinate covariance matrix of the concatenated trajectories of the different solvents as a function of coordinate number. Segments connecting β-sheets and helices are marked by the upper bars. The lower bar indicates the location of the active-site loop.

back on the protein surface, causing the loop Trp55-Asn63 to be pushed against the active site hinge region (Tyr76-Ser82), which causes a slight opening of the active site lid. The observed peak at Ala211 corresponds to the folding back of the loop Leu208-Phe213 to allow the exposure of Pro209 and Pro210 to the nonpolar solvents. As shown in Figs. 5 *b* and 6 *b*, something similar is true for eigenvector 2; the protein shrinks more in cyclohexane, which corresponds to the smaller radius of gyration (Fig. 2). It is noticeable that fluctuations in subspaces spanned by eigenvectors 5–9 are constantly lower in methyl hexanoate than those in water or cyclohexane. Folding back of the loop Leu208-Phe213 creates van der Waals contacts with Pro250-Phe251, resulting in correlated motions between both loops.

Large concerted motions of the active site loop are seen in the subspace spanned by eigenvectors 3 and 4 (see Figs. 5, *c* and *d*, and 6, *c* and *d*). According to Fig. 4 *b*, these motions are somewhat suppressed in cyclohexane. Differences are found in the active-site lid region Arg86-Val97. Fluctuations in this region are only observed in the subspace described by eigenvector 3, which are probably caused by a competition of interactions of hydrophilic groups in the lid (Ser84, Asn87, Asp91, Trp93) between residues on the protein surface and with water. When water is replaced by a hydrophobic solvent, interactions of the hydrophilic groups in the lid with residues on the protein surface are favored, and hence the amount of this motion decreases. Visualization of the C_α motions (Fig. 5) indicates that fluctuations in the loop Ala36-Thr46 are correlated to the motions in the segment Ser56-Thr62. Ala36-Thr46 is located beneath the N-terminal helix, and the turn is at His42. The conformation of this loop is stabilized by a disulfide bridge, and its motion is probably caused by the different hydrophobicity of the loop. The region Ala36-Ile41 is more hydrophobic than the region Cys43-Asp48, which may explain why this motion is also present in methyl hexanoate. It is the competition between residue–solvent molecule and residue–residue interactions that gives rise to these fluctuations. As Ala41 and Thr42 approach the N-terminal helix,

the loop Ser56-Thr62 pushes against the hinge-bending region Phe79-Ser82 of the active site loop, causing a slight displacement of the loop along the long axis of the helix and hence resulting in the fluctuations in the segment Val102-Lys106. A key link in the protein is the segment Gly163-Leu169 connecting two complex structural parts of the enzyme. A plane visualized perpendicular to this loop only crosses the N-terminal helix and the C-terminal region. Motions occurring in the sequence <163 are directly transmitted to the segment >169 and vice versa. Similar effects are seen in the motions along higher eigenvectors (data are not shown), where maximum mean square fluctuations for water and cyclohexane (see Fig. 4 *b*) alternate. Visualization of the motions along these eigenvectors indicates that the differences are caused by distinct fluctuations in the hinge-bending region of the active-site loop (Val102-Gly104) and the region Pro210-Ala212. Fluctuations along the loop are enhanced in water, whereas fluctuations along Pro210-Ala212 predominantly occur in cyclohexane and can be attributed to the hydrophobic nature of this region (Goldsack, 1970). It is interesting to note that the region around Ser103 corresponds to the hinge-bending region of the active-site loop and is close to Gly104, which forms a flexible link between the active-site loop and a short helix. This motion is more pronounced in methyl hexanoate, suggesting that it may be essential in the activation of the Rml.

Continuation of the methyl hexanoate simulation for 200 ps showed that a methyl hexanoate molecule entered the active-site groove during the simulations. This event provides a first insight into the nature and magnitude of the motions occurring during the docking event. The last 200 ps of the first trajectory and the next 200 ps were used for a essential dynamics "combined analysis." Average values of the projections and the mean square fluctuations in these projections of the C_α trajectory onto the combined eigenvectors are shown in Fig. 7. A large difference is observed in the average value of projection of eigenvector 1 corresponding to a conformational change in the loop Val97-Lys106, which is the location where the methyl hexanoate molecule enters the active-site groove (Fig. 10). This is also indicated by the projection of the C_α trajectory onto the eigenvector 1, which is displayed in Fig. 8. At approximately 250 ps a decrease in the value of the dot product is observed, which coincides with the penetration of the hexanoate molecule into the groove. C_α traces of the first eigenvector are shown in Fig. 9. This rearrangement of the loop Val97-Lys106 causes a displacement of the lid, which is damped by the flexible link Gly81. It appears that a hydrogen bond between Gly81 and Asp61 causes the loop Trp55-Thr62 to fold back onto the protein surface. Conformational changes due to the docking event are minor along the eigenvectors that are greater than 1. As shown in Fig. 7 *a*, the average values of the projections are similar for those eigenvectors and smaller than for eigenvector 1. The fluctuations (Fig. 7 *b*) show that all eigenvectors that are in the essential space in the first simulation are also in the essential space of the second, although a rather large shift is observed

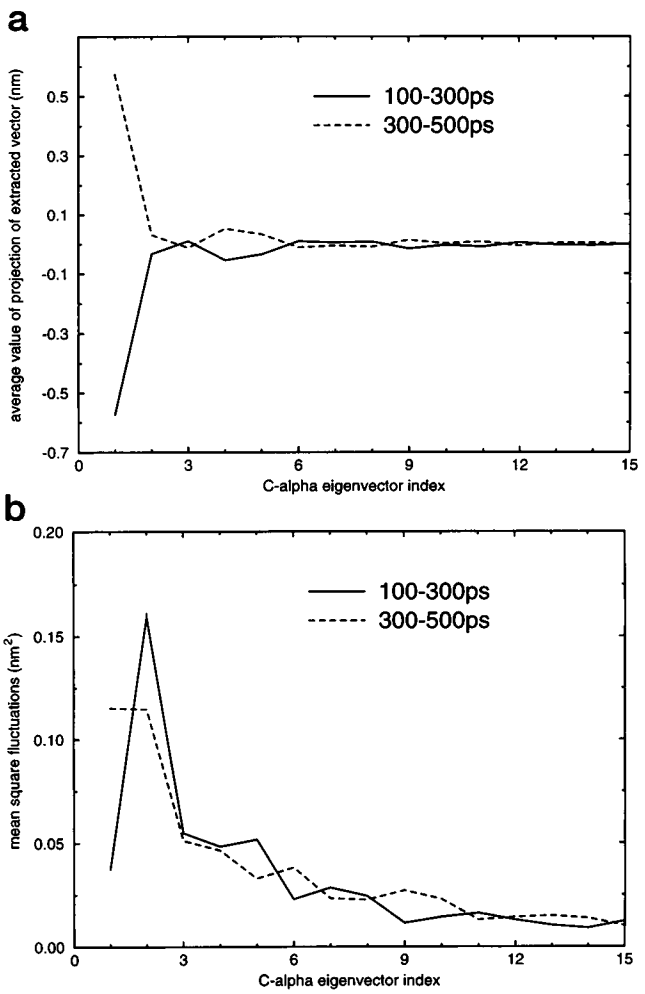

FIGURE 7 (*a*) Average values of the projections of the extracted vectors obtained from the C_α coordinate covariance matrix of Rml in methyl hexanoate as a function of the eigenvector index. (*b*) Mean square fluctuations of the values of the projections of the extracted vectors obtained from the C_α coordinate covariance matrix of Rml in methyl hexanoate as a function of the eigenvector index. Analyses were performed at 200-ps trajectories.

for eigenvector 1. However, eigenvector 1 still shows a considerable fluctuation in the simulation without the methyl hexanoate in the active-site groove, showing it is also part of the essential space. Hence the only significant difference we can observe when methyl hexanoate begins to enter the groove is a shift in structure, as shown in Fig. 7 *a*.

Visualization of the motion along different eigenvectors indicates that fluctuations of the active-site lid and the loops Pro96-Val107 and Asp226-Thr231 are only observed before the methyl hexanoate molecule enters the active-site groove. In both loops, Pro are exposed to the solvent and the observed fluctuations may be caused by the competition between Pro-solvent and Pro-protein interactions. As the substrate enters the groove, these motions are suppressed, whereas motions at Ser98-Lys106 are remarkably increased. The methyl hexanoate molecule enters the active-

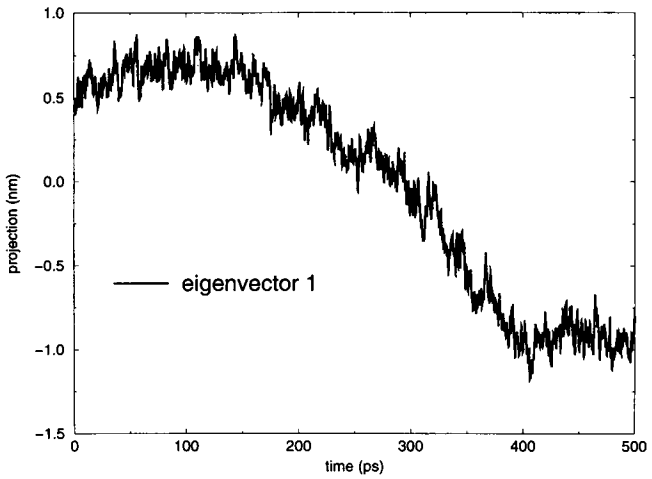

FIGURE 8 Projection of the C_α trajectory onto the eigenvector 1 obtained from the C_α coordinate covariance matrix of Rml in methyl hexanoate plotted against time.

site groove around Pro100, causing a partial opening of the lid in that region. This twist of the lid reduces the fluctuations observed in the region Asp91-Val95. To accommodate the methyl hexanoate molecule, which has in fact been demonstrated to act as a substrate (Norin et al., 1994), fluctuations around Ser98-Lys106 are markedly increased. As the hexanoate molecule further penetrates the groove, the alkyl chain goes beneath Phe94 and essentially pushes this residue upward. This is accompanied by a folding back of Phe213 on the protein surface, providing a "gate" into the active-site groove, as indicated by Fig. 10. This may be the initial step of the opening (roll over) of the lid.

Simulations in nonpolar solvent were performed with the D version of the GROMOS force field, where net charges are replaced by dipoles. To test the effect of the force field on the results, simulations of Rml in methyl hexanoate were carried out with the C version of the GROMOS force field. In this simulation, only internal, buried residues were charged (Arg80, Arg178, Arg196, Asp203, Glu220, and Glu221). Differences between the two simulations in the essential space were deduced from the inner product of the eigenvectors computed from the trajectories of the simulation with the C and D versions of the GROMOS force field. The average inner product of the first 10 eigenvectors of the "C" simulation with the first 10 of the "D" simulation was 0.21. Fig. 11 displays the cross-projections calculated from the first 100 eigenvectors of the two trajectories. These results indicate large differences between the two force fields.

Visualization of the C_α traces indicates that large fluctuations occur in the N-terminus (data not shown) when the C version of the GROMOS force field is used. In particular, fluctuations close to Glu221 are significant, even though Glu220 forms a salt bridge with Arg196, essentially increasing the rigidity.

CONCLUSION

The characteristic of being stable in both aqueous and organic media makes lipases particularly suitable catalysts for a number of synthetic processes. A detailed understanding of the activation mechanism requires the identification of the essential motions in the protein upon activation. We have applied essential dynamics analysis to study the concerted motions in native Rml simulated in water, methyl hexanoate (substrate for Rml), and cyclohexane.

The different solvents have a pronounced effect on the conformational changes and essential motions in the Rml. In nonpolar solvents, the protein shrank slightly, which can be attributed to the folding back of the charged side chains onto the protein surface and an increase in the number of internal hydrogen bonds. The loop Gly35-Ile52, which connects the N-terminus with a β-sheet, folds back on the protein surface. This change is accompanied by a displacement of the loop Trp55-Asn63, which pushes against the active-site hinge region (Tyr76-Ser82) and causes, as a consequence of the van der Waals contacts, a slight opening of the active-site lid. In cyclohexane, the loop Leu208-Phe213 folds back, allowing the exposure of Pro209 and Pro210 to the nonpolar solvent. Our results indicate that fluctuations in the active-site lid (Arg86-Val97) and in the hinge-bending region of the active-site loop (Val102-Gly104) are important in the activation of the Rml. It appears that the latter position is important for the docking of a substrate. During the simulation of the Rml in methyl hexanoate, an ester molecule entered the active-site groove

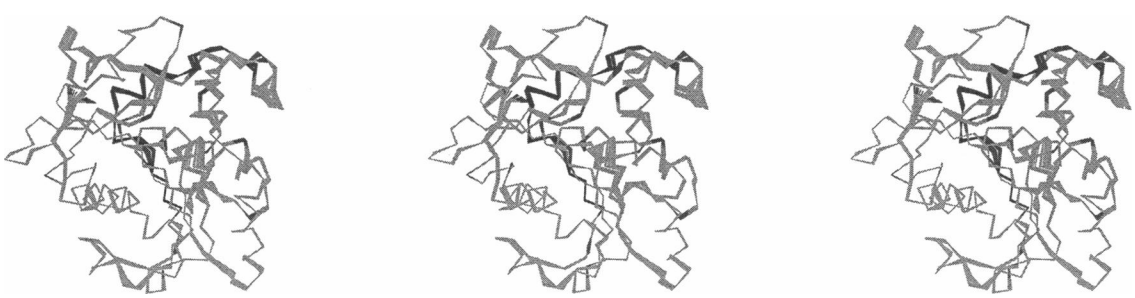

FIGURE 9 Superposition of 10 configurations obtained by projecting the C_α motion onto the first eigenvector. Selected residues and residue numbers are displayed in Fig. 5 *e*. Configurations are separated by 50 ps. See Fig. 5 for more details.

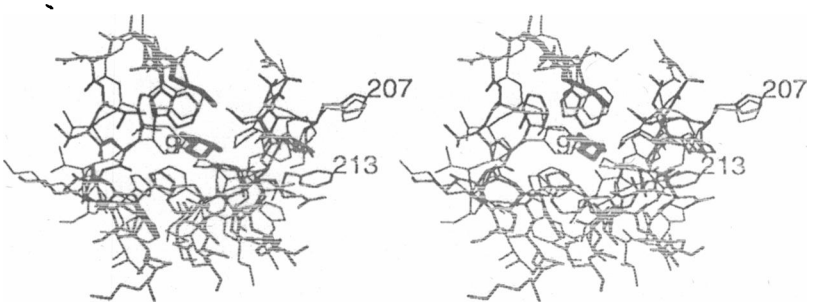

FIGURE 10 Conformational changes in the active-site lid region during the simulation of native Rml in methyl hexanoate. Configurations are taken at 300 ps (*thin lines*) and 500 ps (*thick lines*). The substrate entering the active-site groove is indicated by the thick lines.

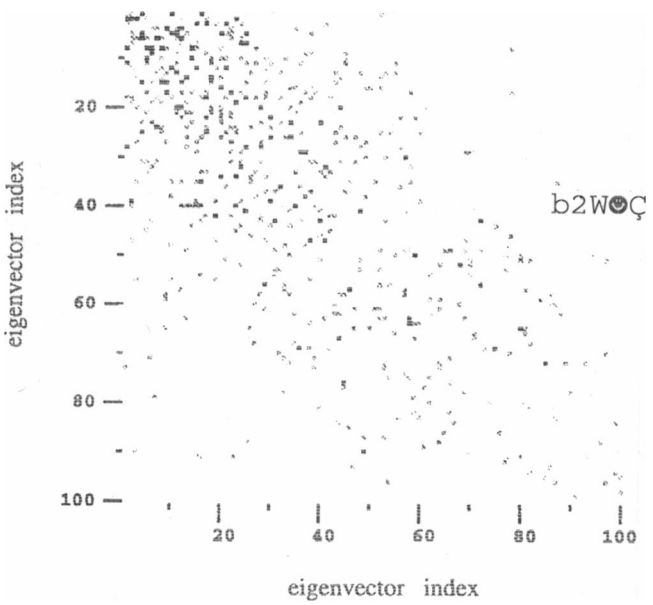

FIGURE 11 Inner products of the first 100 eigenvectors obtained from the C_α coordinate covariance matrix of Rml in methyl hexanoate using the D and C versions of the GROMOS force field.

at this position, which is probably caused by hydrophobic interactions between substrate and residues Pro100 and Pro101. Visualization of several configurations along the trajectory indicated that the alkyl chain of the hexanoate molecule moved under the Phe94, pushing it upward, possibly initiating the activation of the Rml and significantly changing the dynamics of the active-site lid.

Comparison of the methyl hexanoate simulations performed with the GROMOS C and D force fields showed significant effects, as expected from previous studies (van Aalten et al., 1995), with the D force field giving more realistic results than the C force field. The C force field causes a considerable increase in the rigidity of the protein, not allowing enough fluctuation of the lid for a methyl hexanoate molecule to enter the active-site groove. The simulations might be improved by taking into account internal crystal waters, which screen the electrostatic interactions. Another improvement could be the calculation of the actual protonation state of the amino acid residue. Titratable groups that are not stabilized by ion bridges or dipoles probably have perturbed pK_a values in a hydrophobic solvent compared with an aqueous solution.

Computations were performed at Novo-Nordisk A/S.

GHP would like to acknowledge financial support from European grant BIOZ-CT93-5507.

REFERENCES

Aldercreutz, P., and B. Mattiasson. 1987. Aspects of biocatalyst stability in organic solvent. *Biocatalysis.* 1:99–108.

Allen, M. P., and D. J. Tildesley. 1989. Computer Simulation of Liquids. Clarendon, Oxford.

Amadei, A., A. B. M. Linssen, and H. J. C. Berendsen. 1993. Essential dynamics of proteins. *Protein Struct. Funct. Genet.* 17:412–425.

Berendsen, H. J. C., J. R. Grigera, and T. P. Straatsma. 1987. *J. Phys. Chem.* 91:6269–6271.

Bernstein, F. C., T. F. Koetzle, G. J. B. Williams, E. F. Meyer, M. D. Brice, J. R. Rogers, O. Kennard, T. Shimanouchi, and M. Tasumi. 1977. The Protein Data Bank: a computer-based archival file for macromolecular structure. *J. Mol. Biol.* 112:535–542.

Brockman, H. L. 1984. Lipases. B. Bergström and H. L. Brockman, editors. Elsevier Science Publishers, Amsterdam. 1–46.

Brzozowski, A. M., U. Derewenda, Z. S. Derewenda, G. G. Dodson, D. M. Lawson, J. P. Turkenburg, F. Bjorkling, B. Huge-Jensen, S. A. Patkar, and L. Thim. 1991. A model for interfacial activation in lipases from the structure of a fungal lipase-inhibitor complex. *Nature.* 351:491–494.

De Loof, H., L. Nilsson, and R. Rigler. 1992. Molecular dynamics simulations of galanin in aqueous and non-aqueous solution. *J. Am. Chem. Soc.* 114:4028–4035.

Derewenda, U., A. M. Brzozowski, D. M. Lawson, and Z. S. Derewenda. 1992a. Catalysis at the interface: the anatomy of a conformational change in a triglyceride lipase. *Biochemistry.* 31:1532–1541.

Derewenda, U., L. Swenson, Y. Wei, R. Green, P. M. Kobos, R. Joerger, M. J. Haas, and Z. S. Derewenda. 1994. Conformational lability of lipases observed in the absence of an oil-water interface: crystallographic studies of enzymes from the fungi *Humicola lanuginosa* and *Rhizopus delemar*. *J. Lipid Res.* 35:524–534.

Derewenda, Z. S., U. Derewenda, and G. G. Dodson. 1992b. The crystal and molecular structure of the *Rhizomucor miehei* triacylglyceride lipase at 1.9 angstroms resolution. *J. Mol. Biol.* 227:818–839.

Falzone, C. J., P. E. Wright, and S. J. Benkovic. 1994. Dynamics of a flexible loop in dihydrofolate reductase from *Escherichia coli* and its implication for catalysis. *Biochemistry.* 33:439–442.

Fitzpatrick, P. A., A. C. U. Steinmetz, D. Ringe, and A. M. Klibanov. 1993. Enzyme crystal structure in a neat organic solvent. *Proc. Natl. Acad. Sci. USA.* 90:8653–8657.

Goldberg, M., D. Thomas, and M.-D. Legoy. 1990. The control of lipase-catalyzed transesterification and esterification reaction rates. Effects of substrate polarity, water activity and water molecules on enzyme activity. *Eur. J. Biochem.* 190:603–609.

Goldsack, D. E. 1970. Relation of the hydrophobicity index to the thermal stability of homologous proteins. *Biopolymers.* 9:247–252.

Grochulski, P., L. Yunge, J. D. Schrag, F. Bouthillier, P. Smith, D. Harrison, B. Rubin, and M. Cygler. 1993. Insights into interfacial activation from an open structure of *Candida rugosa* lipase. *Biol. Chem.* 268:12843–12847.

Gupta, N. 1991. Thermostabilization of proteins. *Biotechnol. Appl. Biochem.* 14:1–11.

Gupta, N. 1992. Enzyme function in organic solvents. *Eur. J. Biochem.* 203:25–32.

Hartsough, D. S., and M. Merz, Jr. 1993. Protein dynamics and solvation in aqueous and nonaqueous environments. *J. Am. Chem. Soc.* 115: 6529–6537.

Jain, M. K., and O. G. Berg. 1989. The kinetics of interfacial catalysis by phospholipase A_2 and regulation of interfacial activation: hopping versus scooting. *Biochim. Biophys. Acta.* 1002:127–156.

Kabsch, W., and C. Sander. 1983. Dictionary of protein secondary structure: pattern recognition of hydrogen-bonded and geometrical features. *Biopolymers.* 22:2577–2637.

Kempner, E. S. 1993. Movable lobes and flexible loops in proteins. Structural deformations that control biochemical activity. *FEBS Lett.* 326:4–10.

Khmelnitsky, Y. L., A. V. Levashov, N. L. Klyachko, and K. Martinek. 1988. Engineering biocatalytic systems in organic media with low water content. *Enzyme Microb. Technol.* 10:710–724.

Lautz, J., H. Kessler, W. F. van Gunsteren, H.-P. Weber, and R. M. Wenger. 1990. On the dependence of molecular conformation on the type of solvent environment: a molecular dynamics study of cyclosporin A. *Biopolymers.* 29:1669–1687.

Lawson, D. M., A. M. Brzozowski, G. G. Dodson, R. E. Hubbard, B. Huge-Jensen, E. Boel, and Z. S. Derewenda. 1994. The three-dimensional structures of two lipases from filamentous fungi. *In* Lipases—Their Structure, Biochemistry and Application. P. Wooley and S. B. Petersen, editors. Cambridge University Press, New York. 77–94.

Liem, Y. 1992. Computer simulation of liquid lubricants. Ph.D. thesis. University of Manchester, Manchester, England.

Muderhwa, J. M., and H. L. Brockman. 1992. Lateral lipid distribution as a major regulator of lipase activity. *J. Biol. Chem.* 267:24184–24192.

Norin, M., F. Haeffner, K. Hult, and O. Edholm. 1994. Molecular dynamics simulations of an enzyme surrounded by vacuum, water, or a hydrophobic solvent. *Biophys. J.* 67:548–559.

Peters, G. H., O. H. Olsen, A. Svendsen, and R. C. Wade. 1996. Theoretical investigation of the dynamics of the active site lid in *Rhizomucor miehei* lipase. *Biophys. J.* 71:119–129.

Peters, G. H., S. Toxvaerd, N. B. Larsen, T. Bjørnholm, K. Schaumburg, and K. Kjaer. 1995b. Structure and dynamics of lipid monolayers: implications for enzyme catalysed lipolysis. *Nature Struct. Biol.* 2:401–409.

Peters, G. H., S. Toxvaerd, O. H. Olsen, and A. Svendsen. 1995c. Computational studies of activation of lipases and the effect of a hydrophobic environment. *Protein Eng.* 71:119–129.

Philippopoulos, M., Y. Xiang, and C. Lim. 1995. Identifying the mechanism of protein loop closure: a molecular dynamics simulation of the *Bacillus stearothermophilus* LDH loop in solution. *Protein Eng.* 8:565–573.

Piéroni, G., Y. Gargouri, L. Sarda, and R. Verger. 1990. Interactions of lipases with lipid monolayers. Facts and questions. *Adv. Colloid. Interface Sci.* 32:341–378.

Press, W. H., B. P. Flannery, S. A. Teukolsky, and W. T. Vettering. 1987. Numerical Recipes. Cambridge University Press, New York. 357–359.

Ransac, S., C. Riviére, J. M. Soulié, C. Gancet, R. Verger, and G. H. de Haas. 1990. Competitive inhibition of lipolytic enzymes. I. A kinetic model applicable to water-insoluble competitive inhibitors. *Biochim. Biophys. Acta.* 1043:57–66.

Schrag, J. D., and M. Cygler. 1993. 1.8 Å refined structure of the lipase from *Geotrichum candidum. J. Mol. Biol.* 230:575–591.

Thuren, T. 1988. A model for the molecular mechanism of interfacial activation of phospholipase A_2 supporting the substrate theory. *FEBS Lett.* 229:95–99.

van Aalten, D. M. F., A. Amadei, R. Bywater, J. B. C. Findlay, H. J. C. Berendsen, C. Sander, and P. F. W. Stouten. 1996a. A comparison of structural and dynamic properties of different simulation methods applied to SH3. *Biophys. J.* 70:684–692.

van Aalten, D. M. F., A. Amadei, A. B. M. Linssen, V. G. H. Eijsink, and G. Vriend. 1995. The essential dynamics of thermolysin—conformation of the hingebending motion and comparison of simulations in vacuum and water. *Proteins Struct. Funct. Genet.* 22:45–54.

van Aalten, D. M. F., J. B. C. Findlay, A. Amadei, and H. J. C. Berendsen. 1996b. Essential dynamics of the cellular retinol binding protein: evidence for ligand induced conformational changes. *Protein Eng.* 8:1129–1135.

van Gunsteren, W. F., and H. J. C. Berendsen. 1987. GROMOS: Groningen Molecular Simulation Computer Program Package. University of Groningen, Groningen, The Netherlands.

Verger, R., F. Pattus, G. Piéroni, C. Riviere, F. Ferrato, G. Leonardi, and B. Dargent. 1984. Regulation by the interfacial quality of some biological activities. *Colloid. Surf.* 10:163–180.

Vriend, G. 1990. WHAT IF: a molecular modeling and drug design program. *J. Mol. Graph.* 8:52–56.

Vulfson, E. N. 1994. Industrial applications of lipases. *In* Lipases—Their Structure, Biochemistry and Applications. P. Woolley and S. B. Petersen, editors. Cambridge University Press, Cambridge. 271–288.

Wade, R. C., M. E. Davis, B. A. Luty, J. D. Madura, and J. A. McCammon. 1993. Gating of the active site of triose phosphate isomerase: Brownian dynamics simulations of flexible peptide loops in the enzyme. *Biophys. J.* 64:9–15.

Wade, R. C., B. A. Luty, E. Demchuk, J. D. Madura, M. E. Davies, J. M. Briggs, and J. A. McCammon. 1994. Simulation of enzyme-substrate encounter with gated active-sites. *Nature Struct. Biol.* 1:63–67.

Williams, J. C., and A. E. McDermott. 1995. Dynamics of the flexible loop of triosephosphate isomerase: the loop motion is not ligand gated. *Biochemistry.* 34:8309–8319.

Zaks, A., and A. M. Klibanov. 1988. Enzymatic catalysis in nonaqueous solvents. *J. Biol. Chem.* 263:3194–3201.